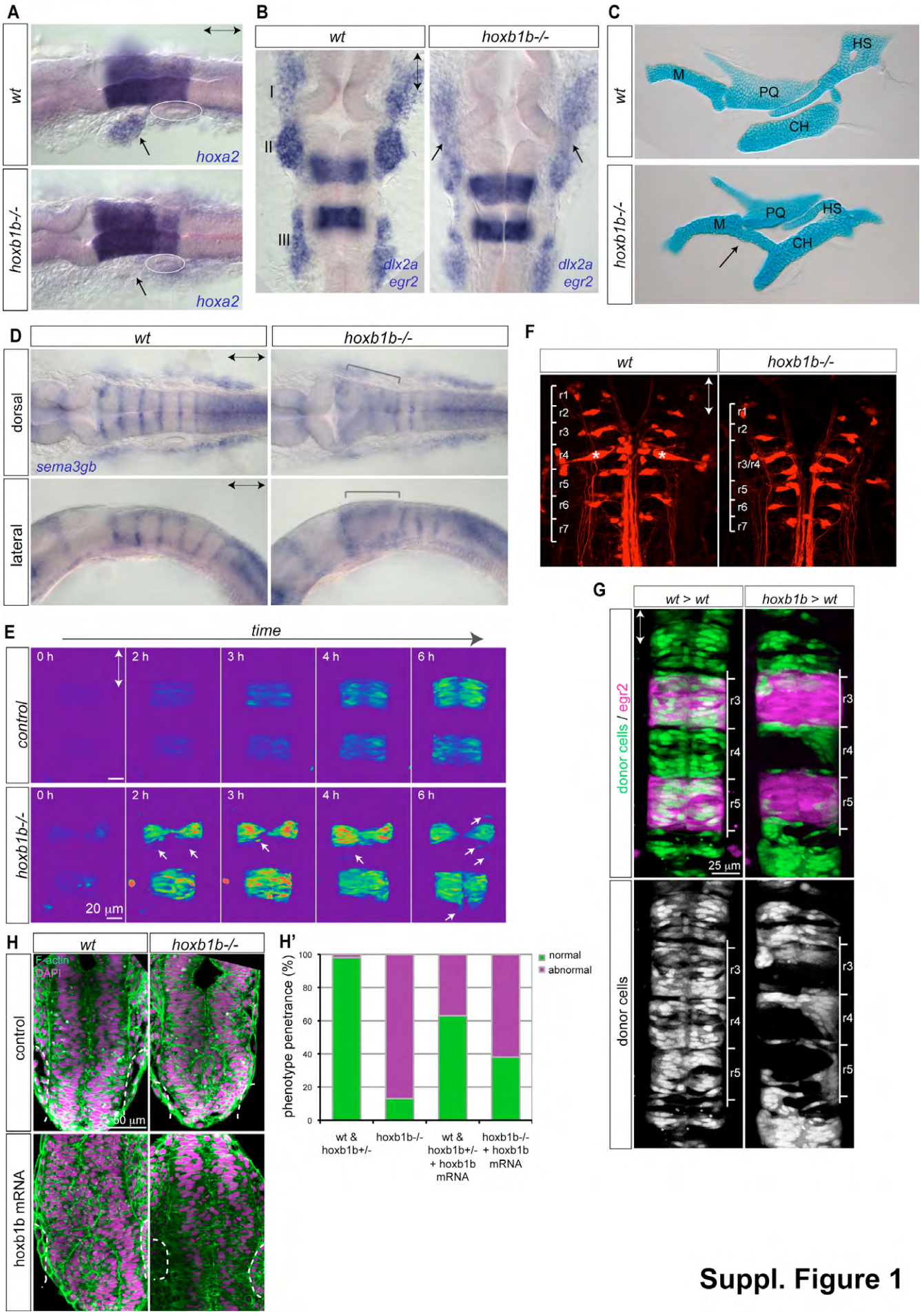

Suppl. Figure 1

Fig. S1: Hindbrain rhombomere identity and boundary formation is disrupted in *hoxb1b*$^{-/-}$ mutant embryos. (A) *In situ* hybridization of *hoxa2* in wild-type and *hoxb1b*$^{-/-}$ embryos at 22hpf. Note lack of *hoxa2* signal in second branchial arch neural crest domains (arrows). Otic vesicles are circled. (B) *In situ* hybridization of *dlx2a* and *egr2* in wild-type and *hoxb1b*$^{-/-}$ at 22hpf with less organized and fused neural crest streams (arrows) in the first (I) and the second (II) arch. (C) Alcian green preparations of branchial jaw cartilages from wild-type and mutant larvae showing single elements: M=Meckel's, PQ=palatoquadrate, CH=ceratohyal, HS=hyosymplectic. Note fusion of first pharyngeal arch Meckel's cartilage and 2nd pharyngeal arch ceratohyal cartilage (arrow). (D) Rhombomere boundary marker *sema3gb* reveals that anterior hindbrain boundaries between r2 and r5 are lost in *hoxb1b*$^{-/-}$ embryos. (E) Onset of *egr2* in r3, r5 of *Tg(egr2b:KalTA4)* live embryos. Start (0h) at about 5 somites. Fluorescence intensity in pseudocolors. Note single *egr2*-positive cells out of register (arrows) in *hoxb1b*$^{-/-}$. (F) Reticulospinal neurons in larval hindbrain demonstrating requirement of Hoxb1b for rhombomere 4-specific Mauthner neurons (asteriks) in r4. (G) Requirement of Hoxb1b in single cells to contribute to anterior r3, r4 hindbrain segments in chimeric embryos. Donor cells from wild-type and *hoxb1b*$^{-/-}$;Tg(h2a.f/z-GFP) donor fluorescent dextran injected embryos (green) transplanted into wild-type *Tg(egr2b:KalTA4)* which expresses mCherry in r3 and r5 (purple). Note sorting out of *hoxb1b*$^{-/-}$ r3, r4 and r5. (H) Anterior lumen morphology at 23hpf upon injection of 750pg *hoxb1b* mRNA per embryo into wild-type (*hoxb1b*$^{+/+}$ and *hoxb1b*$^{+/-}$) (*n*=62) and *hoxb1b*$^{-/-}$)(*n*=21) embryos when compared to control wild-type (*n*=65) and *hoxb1b*$^{-/-}$ (*n*=13) embryos. Anterior-posterior axis marked by double arrows in all panels.

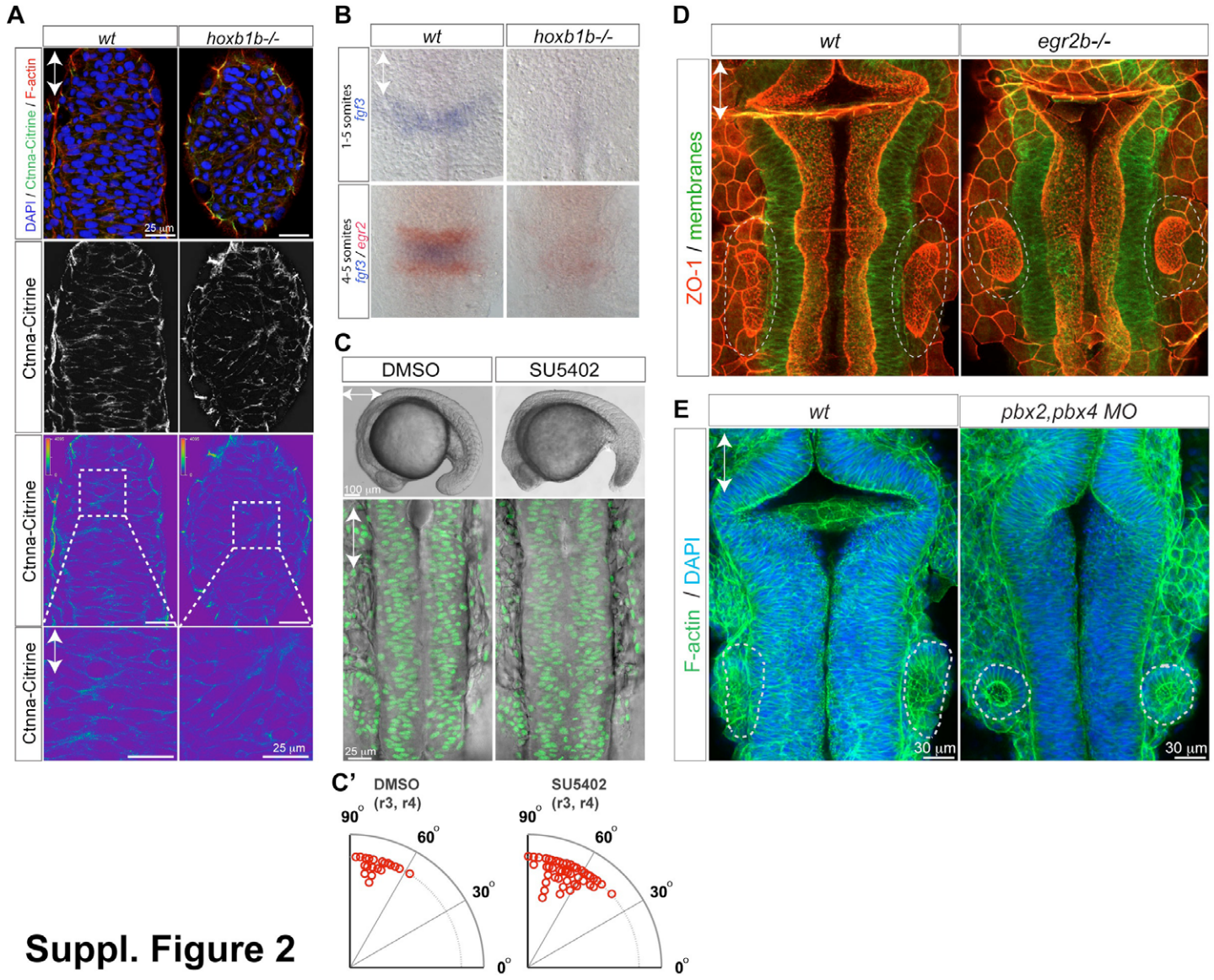

Suppl. Figure 2

Fig. S2: Hindbrain morphogenesis defects in *hoxb1b*$^{-/-}$ mutants is not due to reduced cell-cell adhesion, lack of FGF signaling, or lack of rhombomere boundaries. (A) Ctnna-Citrine (green), F-actin (red) and DNA (blue) in the dorsal neural keel r3/4 level at 15 hpf demonstrating normal levels and distribution of Ctnna in *hoxb1b*$^{-/-}$. Lower panels: Ctnna-Citrine channel shown in pseudocolours. Levels in wild-type and mutant are normalized to the level in the enveloping layer visible in the periphery of the z-section, which is not expected to be affected by *hoxb1b* loss. (B) Decreased expression of *fgf3* mRNA expression (blue) in *hoxb1b*$^{-/-}$ compared to control siblings. (C) Live embyos incubated in SU5402 (100 microM) from the 1 somite stage onward have defective tail outgrowth (top panels) but no defect in hindbrain morphogenesis (lower panels, *Tg(h2a.f/z-GFP)* marks nuclei). (C′) Blocking FGF signaling does not disrupt the predominantly apico-basal orientation of cell division in the neural keel, quantitated as in Fig. 3. (D) Normal hindbrain lumen morphogenesis in 22 hpf egr2−/− embryos based on ZO-1 staining (neuroepithelial apical surface). (E) Normal hindbrain morphology in pbx2;pbx4 double morphants based on phalloidin staining (F-actin) at 21 hpf. Anterior-posterior axis is indicated by double arrows; otic vesicles at the level of r5 are circled by a dashed line.

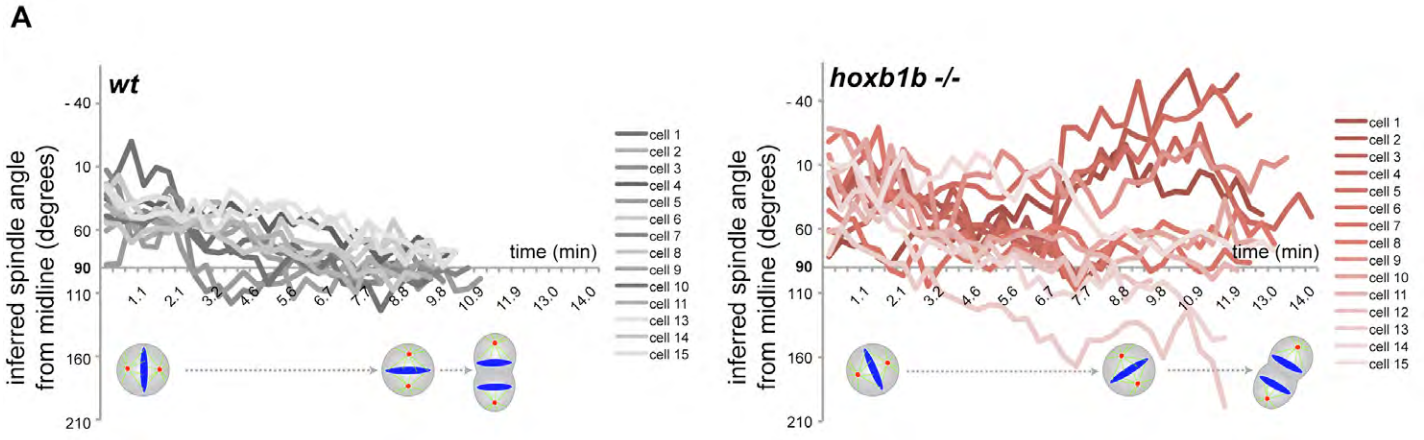

Fig. S3: Hoxb1b is required for the normal rotation of the mitotic spindle during progenitor cell division in the neural keel. (A) Quantitation of metaphase plate rotation in live wild-type (*n*=15 cells, 2 embryos) and *hoxb1b*$^{-/-}$ (*n*=15 cells, 3 embryos) at the neural keel stage (12–15 hpf). Time interval is 21 seconds.

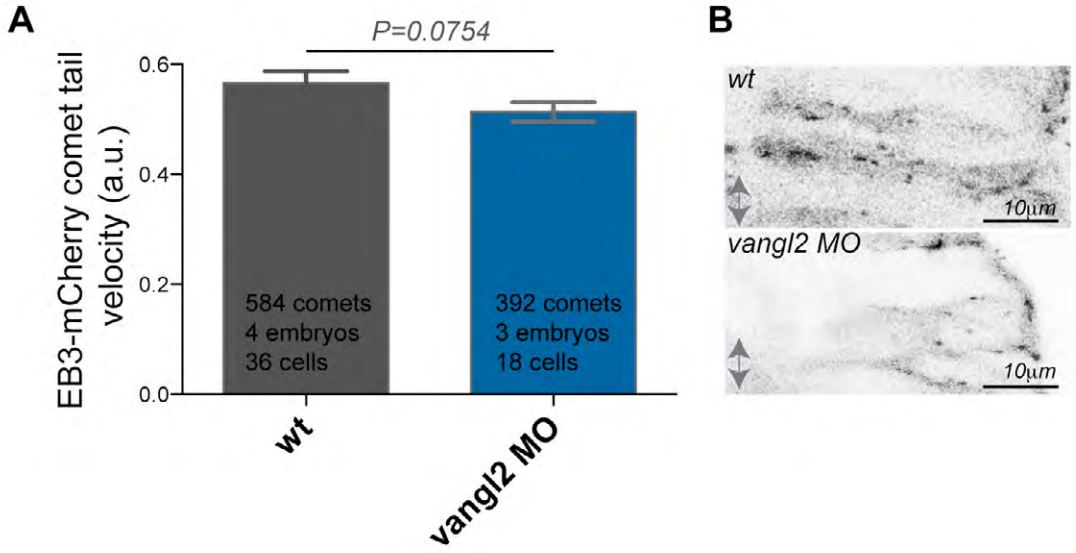

Fig. S4: *Vangl2* loss of function does not impact on plus end MT dynamics. (A) Velocity of EB3-mCherry comets over time in *vangl2* MO injected embryos is not significantly changed when compared to wild-type controls in neural keel hindbrain neuroepithelial cells at 15-17hpf. The data used for quantification of wild-type originates from the same data set as used for the Fig. 5C. (B) Representative pictures of *vangl2* MO injected embryos and wild-type controls injected with EB3-mCherry. Anterior posterior axis is indicated by double arrow, apical is to left, basal to the right.

Movie 1: Neural tube lumen formation in the anterior hindbrain of wild-type (left) and *hoxb1b*$^{-/-}$ (right) transgenic *Gt(Ctnna-Citrine)*^{ct3a} siblings using multiphoton timelapse imaging. Images were acquired every 3 minutes, over 8.05 hours (160 time frames). Beginning at 12 hpf. Note the appearance and gradual accretion of Ctnna-citrine-rich sub-apical surfaces into a single (in wild-type) or multiple (in *hoxb1b*$^{-/-}$ r3/4) lumens. Anterior is to the top, dorsal view.

Movie 2: Cell division behaviour during anterior hindbrain morphogenesis in wild-type (left) and *hoxb1b*$^{-/-}$ (right) siblings, both in the *Tg(h2a.f/z-GFP)* transgenic background. Confocal sections were acquired in time intervals of 21 seconds over 2.6 hours (447 time frames), beginning at 12 hpf. Dorsal view, anterior is to the top.

Movie 3: Tracking of *in vivo* MT plus-end comet kinetics labeled by EB3-GFP in wild-type (left) and *hoxb1b*$^{-/-}$ (right) embryos. Dots mark the position of EB3-GFP puncta at each time-point, lines indicate the history of that EB3 puncta over the course of the timelapse. Movies acquired between 12 and 14 hpf. Anterior is to the top, dorsal view with midline in the center of each frame.